Optica Applicata, Vol. XXI, No. 3, 1991

Comparison of the concentration characteristics of CPC, CCAC, EC and VT

PUNITA TANEJA, T. C. KANDPAL, S. S. MATHUR

Indian Institute of Technology, Centre for Energy Studies, Hauz Khas, New Delhi–110016, India.

The concentration characteristics of a compound parabolic concentrator (CPC) are compared with those of a compound circular arc concentrator (CCAC), an elliptical concentrator (EC) and a V-trough (VT). All these designs use a flat horizontal absorber at the exit aperture. The Monte Carlo ray trace technique is used for the geometrical optical analysis.

1. Introduction

The compound parabolic concentrator belongs to the class of non-imaging solar concentrators [1]–[4]. Such concentrators operate in a seasonally adjusted mode and can achieve the ideal limit of concentration for a given acceptance angle. After the advent of the CPC several other designs have also been proposed to be used as seasonally adjusted linear solar concentrators. Amongst these, the compound circular arc concentrator, the V-trough and the elliptical concentrator have received considerable attention [5]–[10]. Some of these shapes may have the advantage of ease of manufacture with perhaps a minor loss in the optical performance [10]. In the present work, the concentration characteristics of an ideal CPC are compared with those of CCAC, EC and VT using the Monte Carlo ray trace technique. The distribution of local concentration ratio (LCR), over the surface of a flat horizontal (FH) absorber used with a CPC, an EC, a CCAC and a VT of the same height as well as the same sizes of entrance and exit apertures, is studied for different angles of incidence θ of solar radiation on the entrance aperture of the concentrator. The variation of the intercept factor with the angle of incidence for different values of mirror reflectances is plotted for the above concentrator designs. The effect of truncation of the CPC, EC and CCAC on their concentration characteristics has also been investigated.

2. Geometrical-optical design analysis

In an ideal CPC all rays incident at an angle θ, less than the design acceptance angle θ_m, are accepted whereas all rays with θ greater than θ_m are rejected. The maximum concentration ratio C is given by

$$C = 1/\sin\theta_m = D_1/D_2 \tag{1}$$

where D_1 and D_2 denote the diameters of the entrance and exit apertures of the concentrator, respectively. The full height H of the CPC is given by

$$H = \{\cot\theta_m(D_1 + D_2)\}/2. \tag{2}$$

As indicated above, the designs of the CCAC, EC, and VT are so chosen that their heights are the same as that of a CPC given by Eq. (2) and the values of D_1 and D_2 are also the same. To study the concentration characteristics of the above seasonally adjusted linear solar concentrator designs, Monte Carlo ray trace technique is used. For this purpose, the equations of the left and right mirror sections of each design are derived in Cartesian coordinates with origin at the centre of the exit aperture cross-section (point O, in Fig. 1).

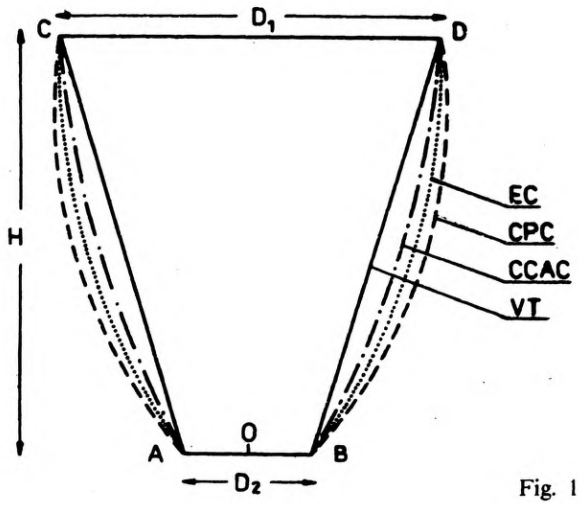

Fig. 1. Cross-section of CPC, CCAC, EC and VT

2.1. Compound parabolic concentrator

The CPC (Fig. 1) has two reflector surfaces which are sections of separate parabolas. The CPC is designed such that the focus of the left parabola lies at the foot of the right parabola and the focus of the right parabola lies at the foot of the left parabola. At the end points of the entrance aperture (points C and D) the slope of the parabolic sections is parallel to the CPC-axis. The angle between the CPC-axis and the axis of either of the parabolas is θ_m.

If the origin of the coordinate system ($X''O''Y''$) be at the vertex O'' of the left parabola (Fig. 2**a**), the equation of the left parabola in this coordinate system can be written as

$$Y'' = bX''^2 \tag{3}$$

where

$$b = 1/4f, \tag{4}$$

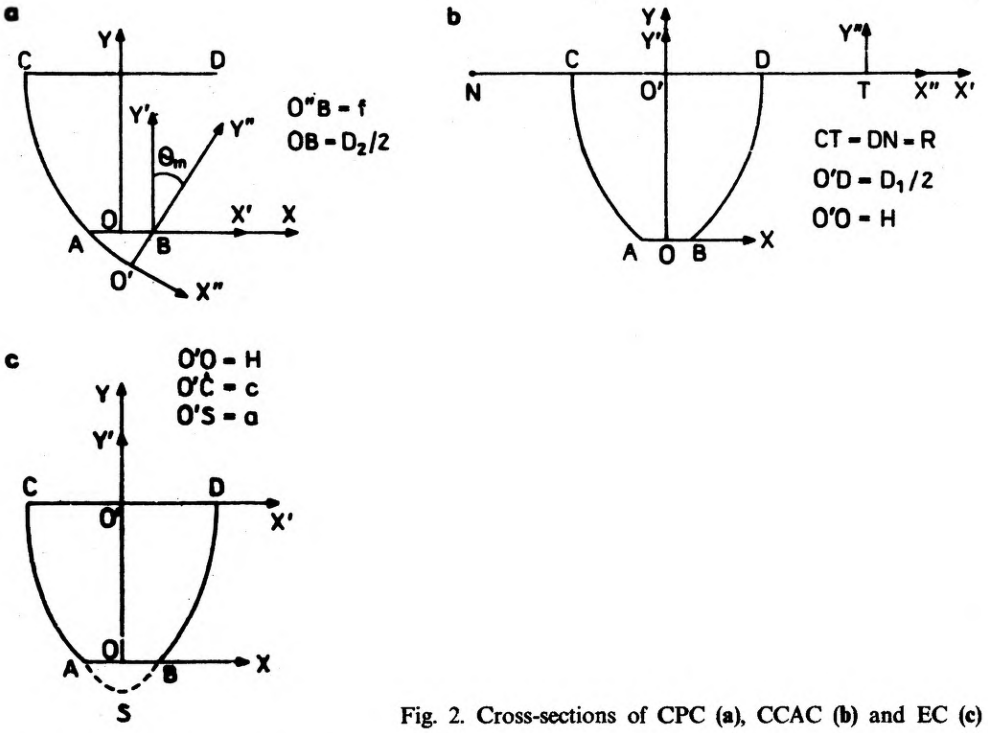

Fig. 2. Cross-sections of CPC (**a**), CCAC (**b**) and EC (**c**)

and the focal length f of the parabola is

$$f = D_2\{1+\sin(\theta_m)\}/2. \tag{5}$$

On shifting the origin O'' to point B (as shown in Fig. 2**a**) by a distance f along the Y''-axis and then rotating the coordinate system by an angle θ_m, the equation of the left parabola with respect to the new coordinate frame $X'BY'$ is

$$b(X'\cos\theta_m - Y'\sin\theta_m)^2 = X'\sin\theta_m + Y'\cos\theta_m + f. \tag{6}$$

Finally, by moving the origin of the coordinate frame $X'BY'$ from point B to the point O, by a distance $D_2/2$ along the X'-axis, the equation of the left parabola with respect to the coordinate frame XOY can be written as

$$(X - D_2/2)\sin\theta_m + Y\cos\theta_m + f = b[(X - D_2/2)\cos\theta_m - Y\sin\theta_m]^2. \tag{7}$$

Since the CPC is symmetric about its axis, a similar procedure can be used to obtain the following equation for the right parabola with respect to the coordinate frame XOY

$$Y\cos\theta_m - (X + D_2/2)\sin\theta_m + f = b[(X + D_2/2)\cos\theta_m + Y\sin\theta_m]^2. \tag{8}$$

2.2. Compound circular arc concentrator (CCAC)

The parabolic sections of the CPC can be approximated by circular corresponding CPC as shown in Fig. 1 [5]. The centre of curvature of each arc is located on the line through the end points of the entrance aperture D_1 (Fig. 2**b**), i.e., the centre of curvature of the left circular arc is located at the point T and that of the right circular arc is located at the point N. This ensures that the tangent to the arcs at the end points of the entrance aperture (points C and D) is parallel to the CPC axis, which is the same condition as that for the CPC. The radii of curvature R of the circular arcs are so chosen that the arcs pass through the end points of the corresponding CPC, i.e., the left circular arc passes through points A and C, whereas the right circular arc passes through the end points B and D (Fig. 1). Consequently, the resulting CCAC has the same height H and entrance and exit aperture diameters (D_1 and D_2), respectively, as that of the ideal CPC.

The radius of curvature can be shown to be given by

$$R = D_1\{(1/\sin^2\theta_m)+(3/\sin\theta_m)+4\}/4. \tag{9}$$

If the origin of the coordinate system ($X''T''Y''$) be at the centre of curvature T of the left circular arc (Fig. 2**b**), the equation of the left circular arc in this coordinate system is given by

$$X''^2 + Y''^2 = R^2. \tag{10}$$

On shifting the origin T to the centre of the entrance aperture (point O') by a distance $(R-D_1/2)$ along the X'' axis, the equation of the left circle with respect to the new coordinate frame $X'O'Y'$ may be written as

$$[X'-(R-D_1/2)]^2 + Y'^2 = R^2. \tag{11}$$

And finally, by shifting the origin of the coordinate frame $X'O'Y'$ by a distance H along the Y' axis from the point O' to the centre of the exit aperture (point O), the equation of the left circular arc with respect to the coordinate frame XOY may be given by

$$(X+D_1/2)^2+(Y-H)^2-2R(X+D_1/2) = 0. \tag{12}$$

Similarly, the equation of the right circular arc with respect to the coordinate frame XOY may be given by

$$(X-D_1/2)^2+(Y-H)^2+2R(X-D_1/2) = 0. \tag{13}$$

2.3. Elliptical concentrator (EC)

The left and right parabolic sections of a CPC may also be approximated by one half of an ellipse, which passes through the end points A, B, C and D of the corresponding CPC (Fig. 1) with the slope of the tangents to the ellipse at the end points of the entrance aperture (points C and D) being parallel to the CPC axis. Thus, the ellipse approximating the CPC is centred at point O' (midpoint of the entrance aperture, Fig. 2**c**) with $O'C$ representing the semiminor axis and $O'S$ representing the

semimajor axis of the ellipse. In the present case

$$a = H\cos\theta_m, \quad c = D_1/2. \tag{14}$$

The equation of the ellipse, with respect to the coordinate frame $X'O'Y'$ with its origin at the centre of the ellipse (point O' in Fig. 2c), is given by

$$X'^2/c^2 + Y'^2/a^2 = 1. \tag{15}$$

On shifting the origin of the coordinate system from the centre of the ellipse (point O') to point O by a distance H along the Y'-axis, the equation of the ellipse with respect to the new coordinate system XOY is

$$X^2/(D_1/2)^2 + (Y-H)^2/(H\cos\theta_m)^2 = 1. \tag{16}$$

2.4. V-trough (VT)

In the case of a V-trough (Fig. 1), two plane mirrors are made to pass through the corresponding end points of the comparable CPC, i.e., one of the plane mirrors passes through the points C and A, whereas the second plane mirror passes through the points D and B. The plane mirrors are inclined at an angle $2\theta_g$ to each other (θ_g being the half groove angle of the V-trough) and have a slant height equal to L. From simple geometrical considerations

$$\theta_g = \tan^{-1}[(D_1 - D_2)/2H], \tag{17}$$

$$L = H/\cos(\theta_g). \tag{18}$$

The equations of the plane mirrors of the VT with respect to the coordinate frame XOY (Fig. 1) can be given by:

$$Y - \{X + D_2/2\}\{\tan(\pi/2 + \theta_g)\} = 0 \quad \text{(left mirror)}, \tag{19}$$

$$Y - \{X - D_2/2\}\{\tan(\pi/2 - \theta_g)\} = 0 \quad \text{(right mirror)}. \tag{20}$$

3. Ray trace evaluation

Monte Carlo ray trace technique is used to study the concentration characteristics of the concentrator-absorber configurations under the following assumptions:

i) The sun is a point source.

ii) The concentrators possess cylindrical symmetry, i.e., the results obtained for one cross-section (in the X-Y plane of Fig. 1) may be extended to the entire length of the concentrator.

The aperture diameter D_1 of the concentrator is divided into a very large number (N = 10,000) of divisions, out of which a representative random sample of n (= 1000) divisions is chosen statistically (one ray is made incident at the centre of each of the n divisions). The path of the rays incident on these n divisions is followed from the point of their incidence on the mirror surface to the point where they are finally intercepted by the absorber surface, or are lost by escaping through the entrance aperture after undergoing reflection(s) on the mirror surfaces. It should be

noted that a certain fraction of the rays incident on the entrance aperture may be intercepted by the absorber directly without striking the mirror surface(s) and the path of such rays is not traced further. The following steps are carried out for the remaining rays that undergo reflection(s) on the mirror surface. All the equations used in the following sections are with respect to the Cartesian coordinate system XOY with its origin at the midpoint of the absorber cross-section (point O, in Fig. 1):

1. Since one ray is made incident on each of the n divisions, the first step is to determine the coordinates (X_j, Y_j) of the point of intersection on the entrance aperture, where the j-th ray making an angle θ with the normal to the aperture plane, hits it. The ray either hits one of the sides of the concentrator or is directly intercepted by the absorber. If the ray is directly intercepted by the absorber then its path is not traced further. On the other hand, if the ray strikes one of the sides of the concentrator, the coordinates of the point of intersection (X_a, Y_a) are obtained by using the appropriate equations of the concentrator(s) (CPC (7), (8), CCAC (12), (13), EC (16), VT (19), (20)) and the equation of the incident ray.

2. In order to determine the angle of incidence of the ray on the surface of the concentrator(s) the slope of the normal (m_1) at the point of incidence on the mirror surface is obtained.

3. The angle of incidence I of the incident ray with the normal at the point (X_a, Y_a) is

$$I = \tan^{-1}\left[\frac{\cot\theta - m_1}{1+\cot\theta(m_1)}\right]. \tag{21}$$

4. The reflected ray at the point (X_a, Y_a) would make an angle $2I$ with the incident ray and its slope m_2 can be calculated accordingly.

5. The coordinates of the point of intersection (X_p, Y_p) of the reflected ray with a flat horizontal absorber are:

$$X_p = (-Y_a + m_2 X_a)/m_2, \tag{22}$$

$$Y_p = 0. \tag{23}$$

6. If the intersection point (X_p, Y_p) lies outside the prespecified dimensions of the absorber then the ray either undergoes second reflection or gets lost by escaping through the entrance aperture.

7. In such a case, once again, the intersection point of the reflected ray with the relevant mirror of the concentrator(s) (left or right) is obtained. If the Y-coordinate of this point is greater than height H of the concentrator then the ray escapes through the entrance aperture, otherwise a second reflection occurs.

8. In case of second/multiple reflection a procedure similar to that used for the case of first reflection is followed and the slope of the reflected ray at the point of second/multiple reflection is obtained. The coordinates of the point of intersection of this ray with the absorber surface are then determined. This procedure is followed till the ray is finally intercepted by the absorber or is lost.

4. Distribution of the local concentration ratio on the surface of the absorber

The local concentration ratio at any point on the absorber surface is defined as the ratio of the flux arriving at that point to the incident flux at the entrance aperture of the solar concentrator. It is used to characterize the uniformity of illumination over the absorber surface. In order to study the distribution of the LCR on the absorber surface, the absorber cross-section is divided into a large number of divisions of equal width. Within the framework of the ray optical model presented in this work, the effective contribution of a ray to the local concentration ratio would depend on: i) the number of reflections $<r>$ the ray undergoes on the mirror surface prior to its interception by the absorber, and ii) the reflectance ρ of the mirror surface. The effective contribution of the ray CI_{eff} can be calculated as

$$CI_{\text{eff}} = \rho^{<r>}. \tag{24}$$

The LCR is calculated as the ratio of the sum of the effective contributions of all the rays intercepted by a typical narrow division of the absorber to the total number of rays incident on a division of equal width in the entrance aperture. A smooth LCR curve is obtained by assigning the LCR of each absorber division to its mid point. The intercept factor is calculated as the ratio of the sum of the effective contribution of all the rays intercepted by the absorber of a chosen size to the total number of rays incident on the entrance aperture.

5. Results and discussion

In order to present a quantitative comparison of the concentration characteristics of the CPC and the other three approximations, some numerical calculations have been made with certain typical values of various design and operational parameters.

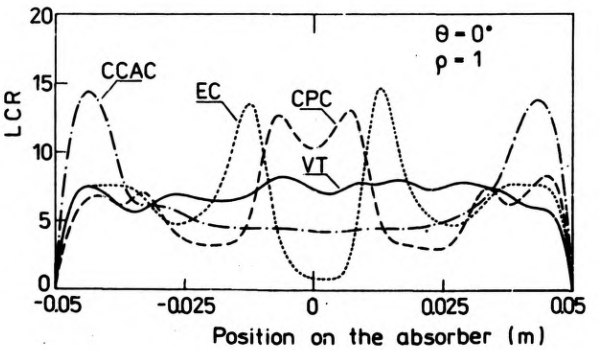

Fig. 3. LCR distribution on the surface of the FH absorber used with a CPC, CCAC, EC and VT, $\theta = 0°$

The CPC has been designed for a θ_m of 8 degrees. The size of the flat horizontal absorber used in all the four designs being compared is 0.10 m.

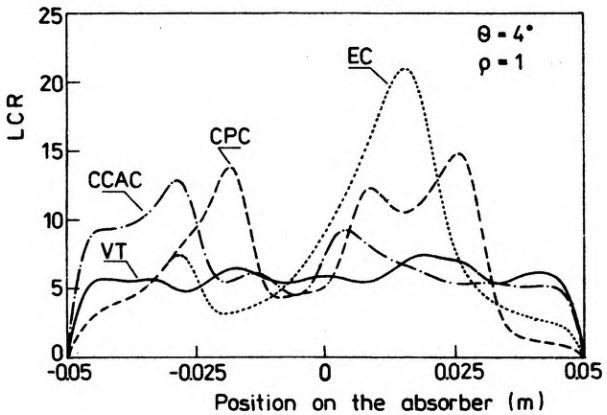

Fig. 4. The same as in Fig. 3, but for $\theta = 4°$

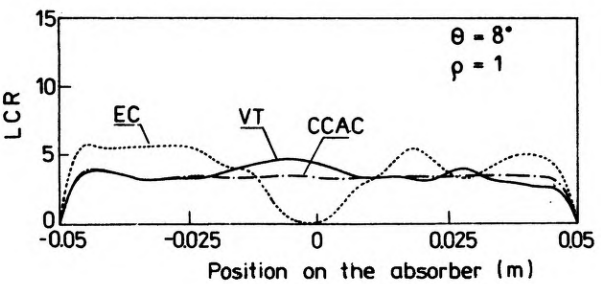

Fig. 5. The same as in Fig. 3, but for $\theta = 8°$

Figures 3–5 show the LCR distribution on the surface of the flat horizontal absorber for θ values of 0, 4 and 8 degrees, respectively. The results shown have been obtained for a mirror reflectance of unity. In Fig. 5, the LCR distribution for the CPC has not been shown as it is well established that for $\theta = \theta_m$, very high LCR at one end of the absorber is observed, thereby making the presentation of the LCR distributions obtained for the CCAC, EC and VT unclear, on the same scale.

Figure 6 depicts the variation of intercept factor with the angle of incidence θ, for an FH absorber. For a CPC, as expected, the intercept factor remains unity for $\theta < \theta_m$ and sharply falls down to zero for $\theta > \theta_m$. For CCAC, EC and VT, the intercept factor remains unity for small angles of incidence, and falls down gradually to zero with an increase in θ. It may be noted that these designs accept a significant number of rays for $\theta > \theta_m$ as well.

Figures 7 and 8 show the variation of the intercept factor for an FH absorber of size 0.10 m with the angle of incidence for mirror reflectance values of 0.8 and 0.6, respectively. With a decrease in the mirror reflectance, there is an overall decrease

in the energy intercepted by the absorber, with all of the designs considered in the present work. This is due to the rays undergoing multiple reflections at the mirror surface(s) prior to their interception by the absorber. However, higher values of the intercept factor for the CCAC as compared to other designs indicate that lesser number of rays undergo multiple reflections in the CCAC for angles of incidence less than 6 degrees. This may also be observed in Fig. 9 which depicts the variation of the average number of reflections undergone by the rays for all the designs considered.

To study the effect of truncating the mirrors on the concentration characteristics, the CPC is first designed for a θ_m of 8 degrees and then approximated by a CCAC and EC of the same height. These designs are then truncated at half their original

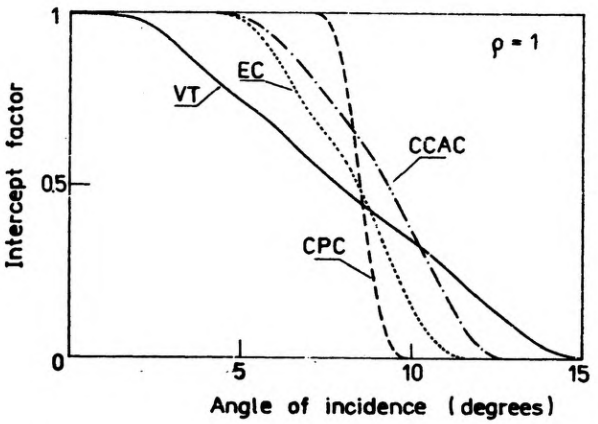

Fig. 6. Intercept factor vs the angle of incidence for an FH absorber used with a CPC, CCAC, EC and VT; $\rho = 1$

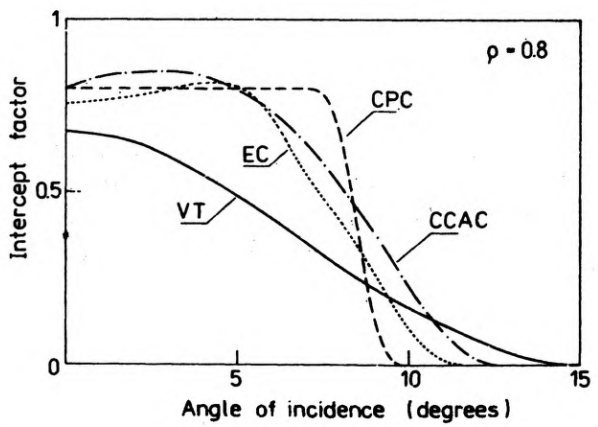

Fig. 7. The same as in Fig. 6, but for $\rho = 0.8$

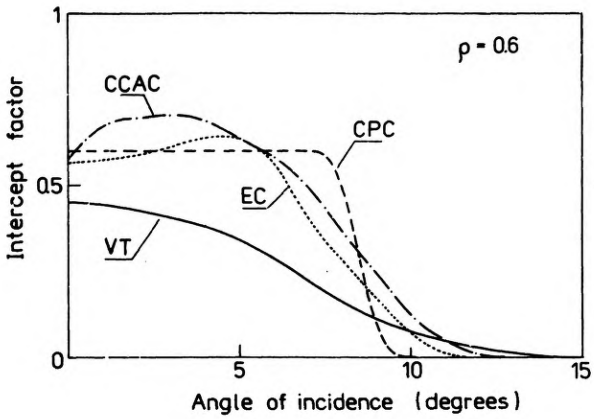

Fig. 8. The same as in Fig. 6, but for $\rho = 0.6$

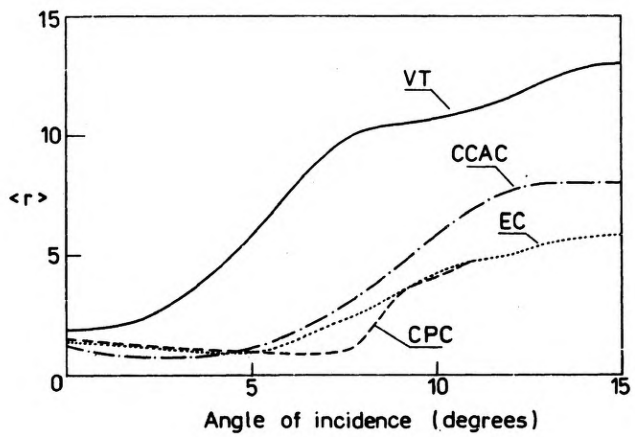

Fig. 9. Average number of reflections vs the angle of incidence for an FH absorber used with a CPC, CCAC, EC and VT

heights and the variation of intercept factor with the angle of incidence θ using a flat horizontal absorber of size 0.10 m is studied as shown in Fig. 10. For these calculations the reflectance of all the mirror surfaces has been taken to be unity. These curves show a similar pattern as those obtained for the full height concentrators.

5. Conclusions

The present work is a part of an ongoing work on the optical concentration characteristics of various seasonally adjusted linear solar concentrators. Further

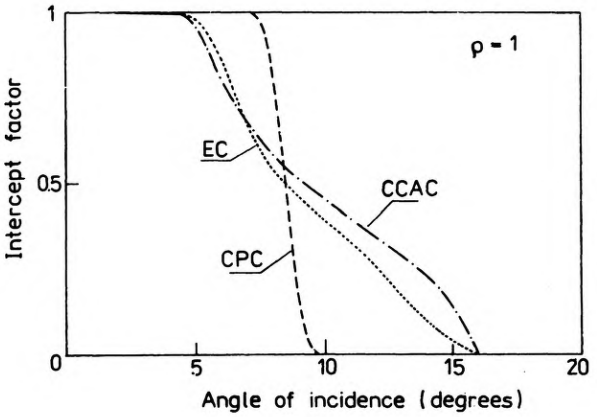

Fig. 10. Intercept factor vs the angle of incidence factor for an FH absorber used with half truncated CPC, CCAC and EC; $\rho = 1$

work is being undertaken to carry out a detailed comparative performance evaluation of various seasonally adjusted designs of linear solar concentrators for their use as primary as well as secondary concentrators in two-stage solar concentrator-receiver systems. The results of the present study indicate that:

i) It is possible to approximate a CPC with a CCAC, an EC and a VT of the same height for a given entrance and exit aperture size.

ii) For mirrors of poor reflectances, the CCAC appears to give a better intercept factor for lower angles of incidence as compared to a CPC.

References

[1] WINSTON R., Solar Energy **16** (1974), 89.
[2] RABL A., GOODMAN N. B., WINSTON R., Solar Energy **22** (1979), 378.
[3] RABL A., Solar Energy **18** (1976), 93.
[4] RABL A., Appl. Opt. **15** (1976), 1871.
[5] JONES R. E., Jr, ANDERSON G. C., Solar Energy **21** (1978), 149.
[6] JONES R. E., Jr, ANDERSON G. C., Solar Energy **25** (1980), 139.
[7] BURKHARD D. G., STROBEL G. L., Appl. Opt. **17** (1978), 1870.
[8] SHAPIRO M. H., Solar Energy **19** (1977), 211.
[9] CANNING J. S., Solar Energy **18** (1976), 155.
[10] GURNEE E. F., Solar Energy **19** (1977), 323.

Received July 18, 1991

Сравнение характеристик для CPC, CCAC, EC и V-T

Характеристики концентрации сложного параболического концентратора (compound parabolic concentrator) сравнены с соответствующими характеристиками сложного колесного дугового концентратора (compound circular arc concentrator), эллиптического концентратора (elliptical

concentrator), а также ввода типа V (V-trough). Все эти конструкции используют горизонтальный абсорбер в выходной апертуре. Применена техника Монте Карло при вычислении хода лучей (ray-tracing) для геометрико-оптического анализа.

Перевел Станислав Ганцаж